Shear-flow-enhanced barrier crossing

Diego Kienle,* Jochen Bammert, and Walter Zimmermann
Theoretische Physik I, Universität Bayreuth, D-95440 Bayreuth, Germany
(Received 21 July 2011; revised manuscript received 20 September 2011; published 18 October 2011)

We consider a single Brownian particle confined in a double well potential (DWP) and investigate its response to a linear shear flow by means of the probability density and current determined via numerical solution of the Fokker-Planck equation. Besides a shear-dependent distortion of the probability distribution, we find that the associated current crossing the potential barrier exhibits a convex dependency on the shear rate when the DWP's minima are far apart. With decreasing distance this functional dependency changes from a convex to concave characteristics accompanied with an increase of the probability current crossing the DWP's barrier. Through the difference map of the particle density distribution it is possible to extract the shear-flow-induced contribution to the particle density driving the barrier-crossing current. This may open the possibility to design specific flow profiles to optimize flow-induced activated transport of nanoparticles.

DOI: 10.1103/PhysRevE.84.042102 PACS number(s): 05.40.−a, 05.10.Gg, 83.50.Ax

The study of the particle dynamics in potential landscapes is of fundamental interest for our understanding of activated transport and plays an important role for many physical systems and processes ranging from chemical reactions [1–3], the folding-unfolding problem of proteins [4–6], to stochastic resonance and synchronization phenomena [7,8], and many more [9–11]. With the advancements to monitor the time-dependent motion of individual polymers and colloidal particles combined with the optical tweezer technique [12–17], it is possible to investigate their steady-state and complex time-dependent behavior [18–30], including positional correlations, and how these are affected by hydrodynamic interaction effects [31–36]. Furthermore, holographic techniques allow experimentalists today to realize even two- and three-dimensional (2D and 3D) optical lattices [37–40], which constitute a 2D and 3D potential landscape for particles undergoing an not necessarily thermally activated transport. Importantly, the magnitude and spatial characteristics of the landscapes can be controlled, so that the design of microfluidic devices with improved efficiency or new functionalities may be designed such as for the sorting of (bio)polymers and colloidal particles according to their mass, particle shape, or refraction index [41–44].

Despite this breadth of quite different physical scenarios, the crossing of an individual (Brownian) particle over a potential barrier may be viewed as the key physical process in activated transport, and is often attributed to Kramers who originally formulated his theory to describe chemical reactions [1]. This theory has been experimentally validated by extracting the transition rates for thermally activated transport from the positional distribution of a single Brownian particle confined in a double-well potential realized through optical tweezers under zero-flow conditions [26]. Of course this distribution is modified under nonequilibrium conditions as in the case of an external flow field where it may adopt an elliptical or parachute-like shape dependent on whether the external flow is a linear shear or Poiseuille, respectively, as recently shown for a single particle within one optical trap [34,45,46]. Importantly, the shape of the distribution does not only depend on the magnitude of the local flow velocity, but also on the (local) shear rate thus affecting the local probability current.

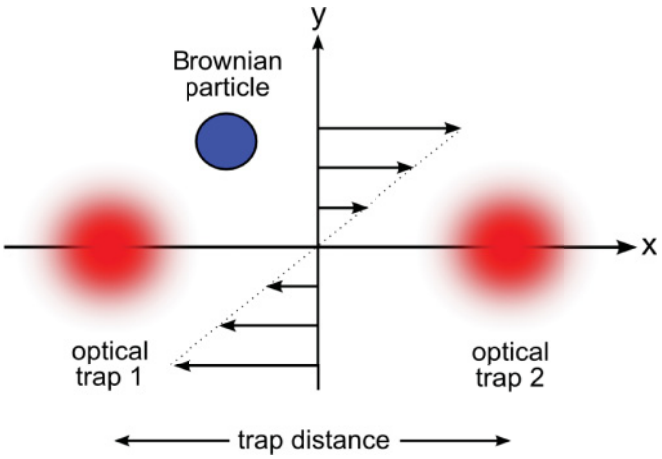

FIG. 1. (Color online) Sketch of the 2D experimental setup: the particle is located within the x-y plane in which it undergoes a random motion. Two (independent) optical traps are used to shape a potential landscape in which the particle is trapped. A linear shear flow is imposed along the connecting line between traps 1 and 2 thus mediating a flow-activated transport between them.

In this Brief Report we extend previous work [26,34,36,45] and investigate the dynamics of a single Brownian particle exposed to constraint forces due to two optical tweezers similar to the experiment of Ref. [26], but in addition impose a linear shear flow as illustrated in Fig. 1 thus introducing an external drag on the particle. By solving the Fokker-Planck equation for the particle distribution it is shown that the external shear mediates a antisymmetric distortion of the probability density and drives a finite particle current across the potential barrier separating the minima of the double-well potential. A proper choice of the potential parameters allows us to tune the curvature of the current as a function of the shear rate from convex to concave characteristics. We introduce difference maps of the particle density to extract the shear-dependent

*Corresponding author: diego.kienle@uni-bayreuth.de

components of the density by which regions with flow-activated transport can be identified.

We model the experimental setup sketched in Fig. 1 consisting of two optical tweezers through a double-well potential (DWP) of the form

$$V(x,y) = \tfrac{1}{2}\kappa\left(y^2 - a_1x^2 + a_2x^4\right), \tag{1}$$

so that the particle is trapped in one of the DWP's minima. κ refers to the spring constant and the two parameters $a_1, a_2 > 0$ determine the position of the two minima and the depth of the DWP. The particle's exposure to a 2D linear shear flow in the x-y plane with the flow direction along the x axis (cf. Fig. 1) is described as

$$\mathbf{u}_0(x,y) = \dot{\gamma}\, y\hat{e}_x \tag{2}$$

with the shear rate $\dot{\gamma}$. Since the DWP and the external flow depend only on the x and y coordinates, the particle's dynamics along the z axis decouples from the former, so that the Brownian dynamics is considered within the x-y plane only. We assume further that the two planar boundaries generating the linear flow profile are sufficiently far away such that the hydrodynamic interaction between the bead and the planes can be neglected.

A particle with radius a embedded in a solvent with viscosity η and temperature T undergoes a thermal motion, which is determined by its diffusion constant $D = k_BT/\zeta$ with the friction coefficient $\zeta = 6\pi\eta a$ and k_B the Boltzmann constant. The shear flow exerts a drag force $\zeta\mathbf{u}_0$ on the particle and together with the potential forces $-\boldsymbol{\nabla}V$ introduces a bias to the random motion. Information about the dynamics of the particle can be obtained from the time evolution of the distribution function for the particle's position which is determined by the Fokker-Planck equation (FPE)

$$\partial_t P(\mathbf{x},t) = -\boldsymbol{\nabla}\cdot\mathbf{j}(\mathbf{x},t) \tag{3}$$

with $\mathbf{j}$ the probability current

$$\mathbf{j}(\mathbf{x},t) = -D\boldsymbol{\nabla}P(\mathbf{x},t) + (\mathbf{u}_0 - \zeta^{-1}\boldsymbol{\nabla}V)P(\mathbf{x},t), \tag{4}$$

and $\mathbf{x} \equiv (x,y)$. For the case considered here, the FPE takes the form

$$\begin{aligned}\partial_t P &= D\Delta P - \dot{\gamma}\, y\partial_x P + \frac{\kappa}{\zeta}\left(6a_2x^2 - a_1 + 1\right)P \\ &\quad + \frac{\kappa}{\zeta}\left[\left(2a_2x^3 - a_1x\right)\partial_x + y\partial_y\right]P.\end{aligned} \tag{5}$$

To proceed it is convenient to rescale space and time through $\mathbf{x} = \delta\tilde{\mathbf{x}}$, respectively, $t = \tau\tilde{t}$ with $\delta^2 = k_BT/\kappa$ and $\tau = \zeta/\kappa$, so that the FPE can be recast in a dimensionless form

$$\begin{aligned}\partial_{\tilde{t}}P &= \tilde{\Delta}P + (3\alpha\tilde{x}^2 - \beta + 1)P \\ &\quad + [(\alpha\tilde{x}^3 - \beta\tilde{x} - \mathrm{Wi}\tilde{y})\partial_{\tilde{x}} + \tilde{y}\partial_{\tilde{y}}]P.\end{aligned} \tag{6}$$

The parameters appearing in Eq. (6) are given by $\alpha = 2\delta^2a_2$, $\beta = a_1$, and $\mathrm{Wi} = b\delta^2/D = \dot{\gamma}\tau$ the Weissenberg number. Using these scaled units the double-well potential [cf. Eq. (1)] can be rewritten in units of k_BT, that is, $V(x,y) = k_BT\tilde{V}(\tilde{x},\tilde{y})$ with

$$\tilde{V} = \tfrac{1}{2}\left(\tilde{y}^2 - \beta\tilde{x}^2 + \alpha\tfrac{1}{2}\tilde{x}^4\right) \tag{7}$$

characterized by two minima $\tilde{x}^{1,2}_{\min} = \pm\sqrt{\beta/\alpha}$ both at $\tilde{y} = 0$ and depth $\tilde{V}_{\min} = |-\alpha\tilde{x}^4_{\min}|/4$. For practical purposes it is more suitable to use these two parameters $\tilde{x}_{\min}$ and $\tilde{V}_{\min}$ instead of α, β to tune the DWP with

$$\alpha = \frac{4|\tilde{V}_{\min}|}{\tilde{x}^4_{\min}}, \quad \beta = \frac{4|\tilde{V}_{\min}|}{\tilde{x}^2_{\min}}. \tag{8}$$

When there is no shear flow applied ($\mathrm{Wi} = 0$), Eq. (6) can be solved analytically

$$P(\tilde{x},\tilde{y}) = P_0e^{-\frac{1}{2}\left[\tilde{y}^2 - \beta\tilde{x}^2 + \frac{1}{2}\alpha\tilde{x}^4\right]} \tag{9}$$

$$P_0 = \sqrt{\frac{2\alpha}{\pi^3\beta}}e^{-z}[I_{-1/4}(z) + I_{1/4}(z)]^{-1} \tag{10}$$

with P_0 the normalization constant, $z = \beta^2/8\alpha$, and I_ν refers to the modified Bessel function of the first kind [47]. The equilibrium particle distribution $P(\tilde{x},\tilde{y})$ is shown in Fig. 2 with the DWP's minima set at $\tilde{x}_{\min} = 3.0$.

At finite shear ($\mathrm{Wi} > 0$), the x-directed shear flow couples the particle's dynamics within the x-y plane through its y dependency [cf. Eq. (2)] and an analytical solution is no longer accessible. In this case we determine $P(\tilde{x},\tilde{y})$ by solving the time-dependent FPE [cf. Eq. (6)] numerically. Figure 3 shows the steady-state, nonequilibrium 2D particle distribution $P(\tilde{x},\tilde{y})$ with a shear rate $\mathrm{Wi} = 2.0$. Contrary to $\mathrm{Wi} = 0$, at finite shear the problem is no longer symmetric with respect to x and y, rather exhibits an inversion-symmetry $P(\tilde{x},\tilde{y}) = P(-\tilde{x},-\tilde{y})$ (cf. Fig. 3) reflecting that the linear shear flow couples the dynamics of the particle along the x and y axis. Furthermore, Fig. 3 shows that the two centers of the distribution $P(\tilde{x},\tilde{y})$ originally located at the minima of the DWP are now displaced toward the lower left, respectively, upper right corner, which is a direct consequence of the inversion symmetry. Simultaneously, the shear flow actuates a nonzero particle current as illustrated by the arrows in Fig. 3 which traverses the potential barrier at $\tilde{x}_{\min} = 0.0$ and thus mediates a exchange of particle density between the two potential minima.

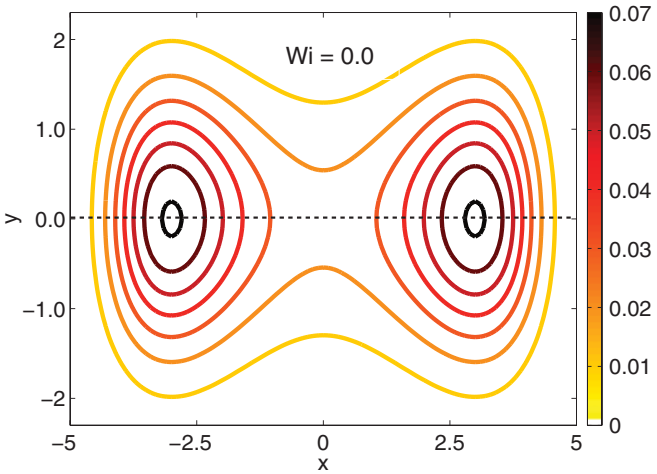

FIG. 2. (Color online) Contour plot of the 2D probability distribution $P(\tilde{x},\tilde{y})$ at equilibrium ($\mathrm{Wi} = 0.0$) with the minima of the DWP at $\tilde{x}_{\min} = 3.0$.

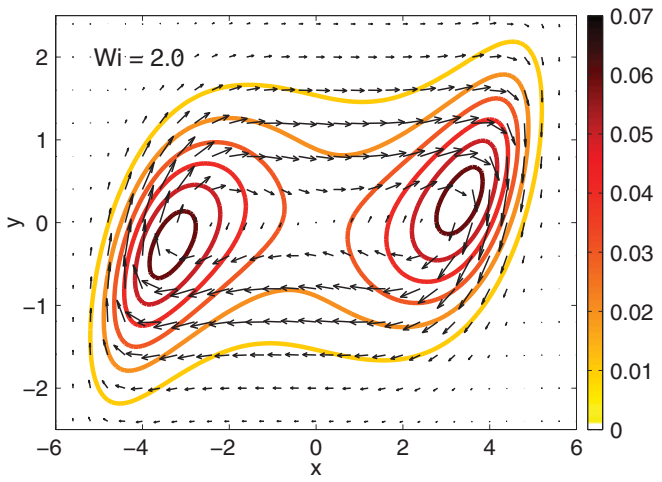

FIG. 3. (Color online) Contour plot of the 2D probability distribution $P(\tilde{x},\tilde{y})$ with $\tilde{x}_{\min} = 3.0$ for a Weissenberg number Wi $= 2.0$. The arrows refer to the probability current $\mathbf{j}(\tilde{x},\tilde{y})$ actuated at finite Wi.

We now vary the shear rate Wi and determine the $\tilde{x}$ component of the effective probability current crossing the potential barrier at $\tilde{x} = 0$ for the upper half-space $\tilde{y} \geqslant 0$ defined by

$$I_0^+ := \int_0^{L_y} d\tilde{y}\, j_{\tilde{x}}(0,\tilde{y}). \tag{11}$$

Figure 4 shows I_0^+ as function of the shear rate Wi for various values of the potential minima $\tilde{x}_{\min}$. When $\tilde{x}_{\min} = 10$ the two minima of the DWP are quite far apart, so that the particle current vanishes for all applied shear rates. With decreasing distance one finds a growing current with increasing shear showing a weak convex behavior at $\tilde{x}_{\min} = 3.0$. Interestingly, the sign of the curvature is reversed and becomes negative (concave) as the two DWP's minima at $\tilde{x}_{\min} = 1.0$ are quite close, so that a finite shear is sufficient to activate the transfer of particles across the barrier separating the two potential minima. At intermediate distance ($\tilde{x}_{\min} = 5.0$) the particle current displays a (weak) S shape as function of Wi, which in turn marks the onset of the sign change in the current from a convex to concave behavior with decreasing distance $\tilde{x}_{\min}$.

In the experiment described in Ref. [26], the effective potential seen by the particle has been extracted from the probability density under zero-flow conditions. When a nonzero flow is applied as discussed here, the question is what is the contribution of the flow to the distortion of the particle distribution. This information can be obtained from the difference between the particle distribution at nonzero shear rate and the one at zero flow, that is, $\Delta P_{\mathrm{Wi}}(\tilde{x},\tilde{y}) = P_{\mathrm{Wi}}(\tilde{x},\tilde{y}) - P_{\mathrm{Wi}=0}(\tilde{x},\tilde{y})$. This is shown in Fig. 5 for the case of a Weissenberg number of Wi $= 2.0$, where the distribution ΔP_{Wi} displays an antisymmetric behavior similar to the one shown in Fig. 3. Clearly visible are the regions with an increased or decreased particle density since the finite shear flow redistributes density away from the DWP's minima, where the distribution $P(\tilde{x},\tilde{y})$ takes its maximum in the absence of flow. Of course, how the shear flow modifies the particle density depends on the position of the minima $\tilde{x}_{\min}$ and on the magnitude of the applied shear rate. Importantly, such difference maps as the one shown in Fig. 5 allow us to spot regions in the particle distribution, which are strongly affected under nonzero flow conditions and thus may provide information about how activated transport can be controlled by external flow fields. Note, the difference map ΔP_{Wi} can be directly determined in experiments using similar techniques as the ones employed in Ref. [26].

In summary, we investigate the dynamics of a single Brownian particle confined within a double-well potential with resemblance to the experiment of Ref. [26], but extended by imposing an additional linear shear flow. Solving the

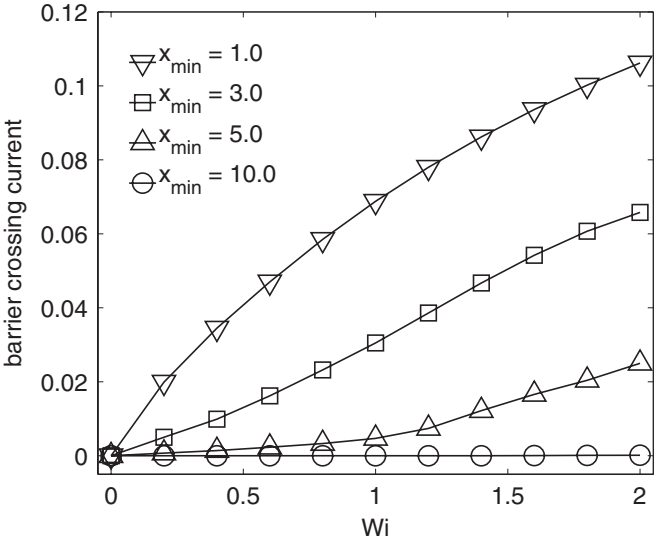

FIG. 4. Probability current I_0^+ obtained by numerically solving Eq. (6) as function of the shear rate Wi and for varying location of the potential minima $\tilde{x}_{\min}$.

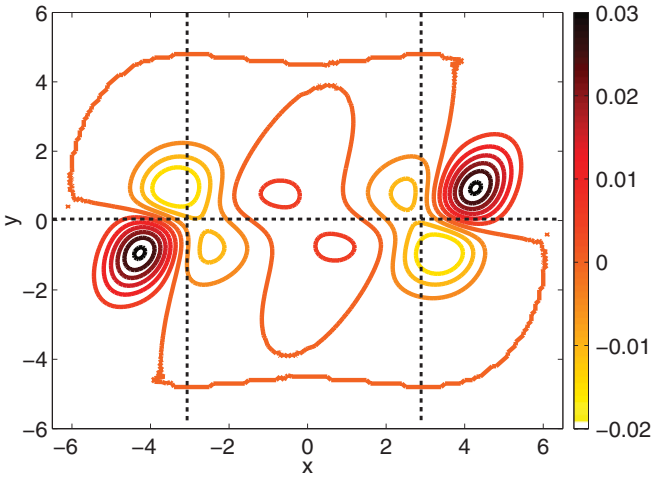

FIG. 5. (Color online) Difference of the particle distribution $\Delta P_{\mathrm{Wi}}(\tilde{x},\tilde{y})$ for a shear rate of Wi $= 2.0$. The crossing points of the dashed lines indicate the location of the minima of the DWP at $\tilde{x}_{\min} = 3.0$.

Fokker-Planck equation for the particle distribution it is shown that the finite shear distorts the distribution driving a particle current across the barrier separating the two minima of the DWP. The particle current shows a convex or concave functional dependency on the Weissenberg number, which can be controlled by the distance between the minima of the double well potential. Furthermore, the inspection of the difference density introduced here using the zero-flow particle density as reference allows to extract those contributions to the particle density, which depend solely on the flow. This information might be useful to understand how external flows of various types affect the distribution of particles as well as the activated transport in inhomogeneous potential landscapes. Utilizing laser-beam optical traps and microfluidic channels, possibly similar to the one used in Ref. [34], the reported behavior may be experimentally probed in a direct manner.

This work has been supported by the German science foundation through FOR608 and SFB 840.

[1] H. A. Kramers, Physica **7**, 284 (1940).
[2] H. C. Brinkman, Physica **22**, 29 (1956); **22**, 149 (1956).
[3] P. Hänggi, P. Talkner, and M. Borkovec, Rev. Mod. Phys. **62**, 251 (1990).
[4] L. Tskhovrebova *et al*., Nature (London) **387**, 308 (1997).
[5] A. D. Mehta *et al*., Science (London) **283**, 1689 (1999).
[6] H. Mayama *et al*., Chem. Phys. Lett. **330**, 361 (2000).
[7] A. Simon and A. Libchaber, Phys. Rev. Lett. **68**, 3375 (1992).
[8] R. Benzi *et al*., SIAM J. Appl. Math. **43**, 565 (1983).
[9] N. G. van Kampen, *Stochastic Processes in Physics and Chemistry* (Elsevier, Amsterdam, 1992).
[10] H. Risken, *The Fokker-Planck Equation*, 2nd ed. (Springer, Berlin, 1996).
[11] C. W. Gardiner, *Handbook of Stochastic Methods*, 3rd ed. (Springer, Berlin, 2004).
[12] A. Ashkin *et al*., Opt. Lett. **11**, 288 (1986).
[13] A. Ashkin, IEEE J. Selected Topics Quantum Electron. **6**, 841 (2000).
[14] K. Dholakia, M. MacDonald, and G. Spalding, Phys. World **15**, 31 (2002).
[15] K. C. Neuman and S. M. Block, Rev. Sci. Instrum. **75**, 2787 (2004).
[16] J. R. Moffitt *et al*., Annu. Rev. Biochem. **77**, 205 (2008).
[17] T. T. Perkins, Laser Photon. Rev. **3**, 203 (2009).
[18] T. T. Perkins *et al*., Science **268**, 83 (1995).
[19] T. T. Perkins, D. E. Smith, and S. Chu, Science **276**, 2016 (1997).
[20] D. E. Smith and S. Chu, Science **281**, 1335 (1998).
[21] D. E. Smith, H. P. Babcock, and S. Chu, Science **283**, 1724 (1999).
[22] P. LeDuc *et al*., Nature (London) **399**, 564 (1999).
[23] P. S. Doyle, B. Ladoux, and J. L. Viovy, Phys. Rev. Lett. **84**, 4769 (2000).
[24] X. R. Bao, H. J. Lee, and S. R. Quake, Phys. Rev. Lett. **91**, 265506 (2003).
[25] R. Delgado-Buscalioni, Phys. Rev. Lett. **96**, 088303 (2006).
[26] L. I. McCann, M. Dykman, and B. Golding, Nature (London) **402**, 785 (1999).
[27] E. R. Dufresne, T. M. Squires, M. P. Brenner, and D. G. Grier, Phys. Rev. Lett. **85**, 3317 (2000).
[28] S. A. Tatarkova, W. Sibbett, and K. Dholakia, Phys. Rev. Lett. **91**, 038101 (2003).
[29] P. Wu, R. Huang, C. Tischer, A. Jonas, and E.-L. Florin, Phys. Rev. Lett. **103**, 108101 (2009).
[30] D. Wu *et al*., Phys. Rev. Lett. **103**, 050603 (2009).
[31] J.-C. Meiners and S. R. Quake, Phys. Rev. Lett. **82**, 2211 (1999).
[32] S. Martin, M. Reichert, H. Stark, and T. Gisler, Phys. Rev. Lett. **97**, 248301 (2006).
[33] M. Atakhorrami, K. M. Addas, and C. F. Schmidt, Rev. Sci. Instrum. **79**, 043103 (2008).
[34] A. Ziehl, J. Bammert, L. Holzer, C. Wagner, and W. Zimmermann, Phys. Rev. Lett. **103**, 230602 (2009).
[35] J. Kotar *et al*., Proc. Natl. Acad. Sci. USA **107**, 7669 (2010).
[36] L. Holzer, J. Bammert, R. Rzehak, and W. Zimmermann, Phys. Rev. E **81**, 041124 (2010).
[37] P. T. Korda, M. B. Taylor, and D. G. Grier, Phys. Rev. Lett. **89**, 128301 (2002).
[38] M. P. MacDonald *et al*., Science **296**, 1101 (2002).
[39] E. R. Dufresne *et al*., Rev. Sci. Instrum. **72**, 1810 (2001).
[40] J. E. Curtis, B. A. Koss, and D. G. Grier, Opt. Commun. **207**, 169 (2002).
[41] J. Han and H. G. Craighead, Science **288**, 1026 (2000).
[42] M. P. MacDonald, G. C. Spalding, and K. Dholakia, Nature (London) **426**, 421 (2003).
[43] K. Ladavac, K. Kasza, and D. G. Grier, Phys. Rev. E **70**, 010901(R) (2004).
[44] L. Paterson *et al*., Appl. Phys. Lett. **87**, 123901 (2005).
[45] J. Bammert and W. Zimmermann, Phys. Rev. E **82**, 052102 (2010).
[46] J. Bammert, L. Holzer, and W. Zimmermann, Eur. Phys. J. E **33**, 313 (2010).
[47] M. Abramowitz and I. Stegun, *Handbook of Mathematical Functions* (Dover, New York, 1965).